Long-time entanglement in the Quantum Walk

Gonzalo Abal[1], **Raul Donangelo**[2], **Hugo Fort**[3]

[1]Instituto de Física, Facultad de Ingeniería,
Universidad de la República, C.C. 30, C.P. 11000, Montevideo, Uruguay

[2]Instituto de Física, Universidade Federal do Rio de Janeiro (UFRJ),
C.P. 68528, Rio de Janeiro 21941-972, Brazil

[3]Instituto de Física, Facultad de Ciencias.
Universidad de la República, C.P. 11400, Montevideo, Uruguay

abal@fing.edu.uy, donangel@if.ufrj.br, hugo@fisica.edu.uy

Abstract. *The coin-position entanglement generated by the evolution operator of a discrete–time quantum walk is quantified, using the von Neumann entropy of the reduced density operator (entropy of entanglement). In the case of a single walker, the entropy of entanglement converges, in the long time limit, to a well defined value which depends on the initial state. Exact expressions are obtained for local and non-local initial conditions. We also discuss the asymptotic bi-partite entanglement generated by non-separable coin operations for two coherent quantum walkers. In this case, the entropy of entanglement is observed to increase logarithmically with time.*

1. Introduction

The discrete-time Quantum Walk (QW), first introduced in by Aharonov, Davidovich and Zagury [1], is a quantum analog for the classical random walk where the classical coin flipping is replaced by a unitary operation in a one-qubit Hilbert space. Quantum walks in several topologies [2] have been used as the basis for optimal quantum search algorithms [3, 4] which take advantage of quantum entanglement and parallelism. Entanglement is an essential resource in many quantum information processing protocols, such as teleportation, secure key distribution or even Shor's factorization algorithm [5]. For pure bi-partite states, it can be quantified using the von Neumann entropy of the reduced density operator (henceforth, the entropy of entanglement S_E).

The evolution operator of a QW generates quantum correlations between the "coin" and position degrees of freedom. This entanglement can be quantified in the long time limit [6] where exact expressions for S_E can be obtained, for given initial conditions. When two quantum walkers are considered, different kinds of bi-partite entanglement may appear. We shall discuss this situation and include some preliminary results for QWs with non-separable coin operators.

This work is organized as follows. In Section 2, we briefly review the discrete-time quantum walk on the line and define the entropy of entanglement. The dependence of the asymptotic entanglement for (i) localized initial conditions and (ii) non-local initial conditions spanned by the position eigenstates $|\pm 1\rangle$ are discussed. Section 3 is devoted to the case of two quantum walkers. Finally, in Section 4 we summarize our conclusions and discuss future developments.

2. Quantum walk on the line

A step of the QW is a conditional translation between discrete sites on a line. The Hilbert space is the tensor product of two subspaces, $\mathcal{H} = \mathcal{H}_P \otimes \mathcal{H}_C$. The first part, $\mathcal{H}_P$, is a quantum register spanned by the eigenstates of the position operator, $X\|x\rangle = x\|x\rangle$, with x an integer label. The second part, $\mathcal{H}_C$, is a single-qubit "coin" subspace spanned by two orthonormal states denoted $\{|0\rangle, |1\rangle\}$. To avoid confusion, we use the symbol $\|\cdot\rangle$ to indicate states in $\mathcal{H}_\mathcal{P}$. A generic state for the walker is

$$|\Psi\rangle = \sum_{x=-\infty}^{\infty} \|x\rangle \otimes [a_x|0\rangle + b_x|1\rangle] \tag{1}$$

in terms of complex coefficients satisfying $\sum_x |a_x^2| + |b_x|^2 = 1$ (in what follows, the summation limits are left implicit).

The evolution of the walk is described by the unitary operator

$$U = S \cdot (I_P \otimes U_C) \tag{2}$$

where U_C is a unitary operation in $\mathcal{H}_C$ and I_P is the identity in $\mathcal{H}_P$. A convenient choice for U_C is a Hadamard operation, defined by $H|0\rangle = (|0\rangle + |1\rangle)/\sqrt{2}$ and $H|1\rangle = (|0\rangle - |1\rangle)/\sqrt{2}$. When $U_C = H$ one refers to the process as a Hadamard walk. The shift operator

$$S = \sum_x \{\|x+1\rangle\langle x\| \otimes |0\rangle\langle 0| + \|x-1\rangle\langle x\| \otimes |1\rangle\langle 1|\} \tag{3}$$

conditionally changes the position one step to the right for $|0\rangle$ or to the left for $|1\rangle$. This conditional shift entangles the coin and position of the quantum walker.

In terms of the density operator, $\rho = |\Psi\rangle\langle\Psi|$, the evolution is given by $\rho(t) = U^t \rho(0)\, U^{\dagger\, t}$ where the non-negative integer t counts the discrete time steps that have been taken. The probability distribution for finding the walker at site x at time t is $P(x,t) = tr(\rho P_x) = |a_x|^2 + |b_x|^2$, where $P_x = \|x\rangle\langle x\| \otimes I_c$. The variance of this distribution increases quadratically with time as opposed to the classical random walk, in which the increase is only linear. This property depends on quantum coherence and is lost in the presence of noise [7, 8].

For pure, bi-partite states, entanglement can be quantified by the Entropy of Entanglement [9, 10], defined as the von Neumann entropy of the reduced density operator. If the partial trace is conveniently taken over the position subspace, $\rho_c = tr_x(\rho)$, and

$$S_E \equiv -tr(\rho_c \log_2 \rho_c). \tag{4}$$

This quantity is zero for a product state, unity for a maximally entangled state and it is invariant under LOCC (local operations with classical communication) [11, 12].

In an early paper, Nayak and Vishwanath [13] have shown that Fourier analysis may be used to obtain long-time asymptotic expressions for the amplitudes $a_x(t)$ and $b_x(t)$, for given initial conditions. We used this approach to characterize the asymptotic entanglement of the QW in [6]. In the rest of this Section, we summarize and extend those results.

We start by defining the dual space, $\tilde{\mathcal{H}}_k$, spanned by the Fourier transformed kets $|k\rangle = \sum_x e^{ikx}|x\rangle$, with real wavenumbers $k \in [-\pi, \pi]$. In this representation the state vector is

$$|\Psi\rangle = \int_{-\pi}^{\pi} \frac{dk}{2\pi} |k\rangle \otimes \left[\tilde{a}_k|0\rangle + \tilde{b}_k|1\rangle\right]. \tag{5}$$

of the QW, ,

These amplitudes are related to the position amplitudes in eq. (1) by $\tilde{a}_k = \sum_x e^{-ikx} a_x$ and $\tilde{b}_k = \sum_x e^{-ikx} b_x$, respectively. Since the step size is constant, the shift operator defined in eq. (3)

$$U_k = \frac{1}{\sqrt{2}} \begin{pmatrix} e^{-ik} & e^{-ik} \\ e^{ik} & -e^{ik} \end{pmatrix}. \tag{6}$$

is diagonal in k. Then, if $|\Phi_k\rangle$ is the spinor $(\tilde{a}_k, \tilde{b}_k)^T$, the time evolution of an initial state can be expressed as

$$|\Phi_k(t)\rangle = U_k^t |\Phi_k(0)\rangle = e^{-i\omega_k t}\langle\varphi_k^{(1)}|\Phi_k(0)\rangle\ |\varphi_k^{(1)}\rangle + (-1)^t e^{i\omega_k t}\langle\varphi_k^{(2)}|\Phi_k(0)\rangle\ |\varphi_k^{(2)}\rangle. \tag{7}$$

where $|\varphi_k^{(1,2)}\rangle$ are the eigenvectors and $\pm e^{\mp i\omega_k}$ the eigenvalues of U_k and the angle $\omega_k \in [-\pi/2, \pi/2]$ is defined by $\sin\omega_k \equiv \sin k/\sqrt{2}$. In principle, eq. (7) may be transformed back to position space and the probability distribution $P(x,t)$ obtained implicitly in terms of complicated integrals which, for arbitrary times, can only be done numerically. However, in the long time limit, approximate stationary phase methods can be used to evaluate these integrals for given initial conditions [13]. We may avoid these technical difficulties, because the asymptotic entanglement S_E may be obtained directly from eq. (7) and there is no need to transform back to position space.

The entropy of entanglement of a quantum walker can be obtained after diagonalisation of the reduced density operator

$$\rho_c = tr_x(\rho) = \begin{pmatrix} A & B \\ B^* & C \end{pmatrix}, \tag{8}$$

where

$$\begin{aligned} A &\equiv \sum_x |a_x|^2 = \int_{-\pi}^{\pi} \frac{dk}{2\pi} |\tilde{a}_k|^2 \\ B &\equiv \sum_x a_x b_x^* = \int_{-\pi}^{\pi} \frac{dk}{2\pi} \tilde{a}_k \tilde{b}_k^* \\ C &\equiv \sum_x |b_x|^2 = \int_{-\pi}^{\pi} \frac{dk}{2\pi} |\tilde{b}_k|^2. \end{aligned} \tag{9}$$

Normalization requires that $\mathrm{tr}(\rho) = A + C = 1$. In terms of

$$\Delta \equiv AC - |B|^2 \tag{10}$$

the real, positive eigenvalues of ρ_c are $r = \frac{1}{2}\left[1 + \sqrt{1 - 4\Delta}\right]$ and $1 - r$. The entropy of entanglement is obtained from $S_E = -r\log_2 r - (1-r)\log_2(1-r)$. The units for bi-partite entanglement are e-bits, or entanglement bits, where one e-bit is the amount of entanglement contained in a Bell pair. The determinant $\Delta \in [0, 1/4]$ contains all the information required to quantify the coin-position entanglement in the QW. The greater the value of Δ, the greater the entanglement.

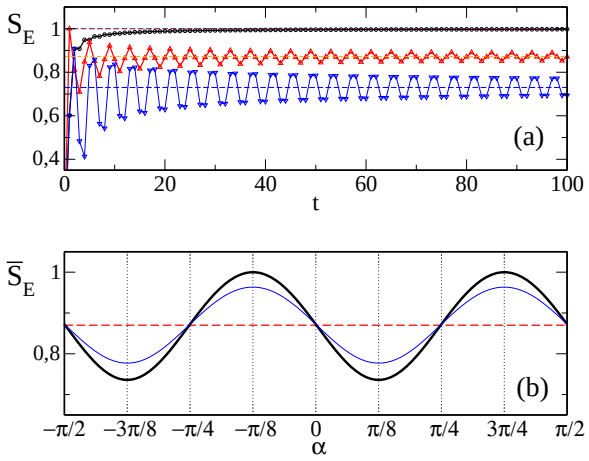

Figure 1. (color online) Entanglement vs discrete time for localized initial states with coin states $|\chi\rangle$ parametrized in eq. (11); (a) time evolution of the entropy of entanglement S_E for $\alpha = -\pi/8$ and $\beta = \pi$ (black, full asymptotic entanglement), $\beta = \pi/2$ (red, intermediate asymptotic entanglement) and $\beta = 0$, (blue, minimimum asymptotic entanglement); (b) asymptotic entropy of entanglement $\bar{S}_E$ vs α from eq. (12) for $\beta = 0$ (thick black line) $\beta = \pi/4$, (thin blue line) and $\beta = \pm\pi/2$ (dashed red line).

2.1. Local initial coins

Consider a localized initial state ($x = 0$, without loss of generality) with an arbitrary coin parametrized in terms of two real angles $\alpha \in [-\pi/2, \pi/2]$ and $\beta \in [-\pi, \pi]$,

$$|\chi\rangle \equiv \frac{1}{\sqrt{2}} \left[\cos\alpha|0\rangle + e^{i\beta}\sin\alpha|1\rangle\right]. \tag{11}$$

In this case, the Fourier-transformed coefficients appearing in eq. (5) are $\tilde{a}_0(0) = \cos\alpha$, $\tilde{b}_0(0) = e^{i\beta}\sin\alpha$ and $\tilde{a}_k(0) = \tilde{b}_k(0) = 0$ for $k \neq 0$. The integrands in eqs. (9) can be calculated from eq. (7) in terms of α and β. For long times, $t \gg 1$, the k-averages in eqs. (9) are time-independent and the dependence of Δ on the initial coin is

$$\bar{\Delta} \equiv \lim_{t\gg 1} \Delta = \Delta_0 - 2b_1^2 \cos\beta \sin(4\alpha), \tag{12}$$

with $\Delta_0 = (\sqrt{2}-1)/2$ and $b_1 = (2-\sqrt{2})/4$. The details of the calculation leading to this expression can be found in Appendix A of Ref. [6] and will not be reproduced here. In panel (a) of Fig. 1 the time evolution of the entropy of entaglement is shown for fixed $\alpha = -\pi/8$ and $\beta = \pi, \pi/2, 0$ for which the asymptotic entanglement is maximum, intermediate or minimum respectively. In particular, the intermediate asymptotic entanglement level, $\bar{S}_E \approx 0.872$, has been erroneously reported as generic (i.e. resulting from *all* initial coins) in Ref. [14]. In fact, as follows from expression (9), it is obtained for arbitrary α only if $\beta = \pi/2$. Also apparent from Fig. 1 is the fact that lower entanglement levels result in larger oscillations and have a slower convergence to their asymptotic values. Panel (b) of this figure shows the variation of the asymptotic entanglement with α for three values of the relative phase β. For localized initial coins the minimum asymptotic entanglement is $\bar{S}_E \approx 0.736$. However, as we discuss next, if non-local initial conditions are considered, arbitrary low values for asymptotic entanglement may be obtained.

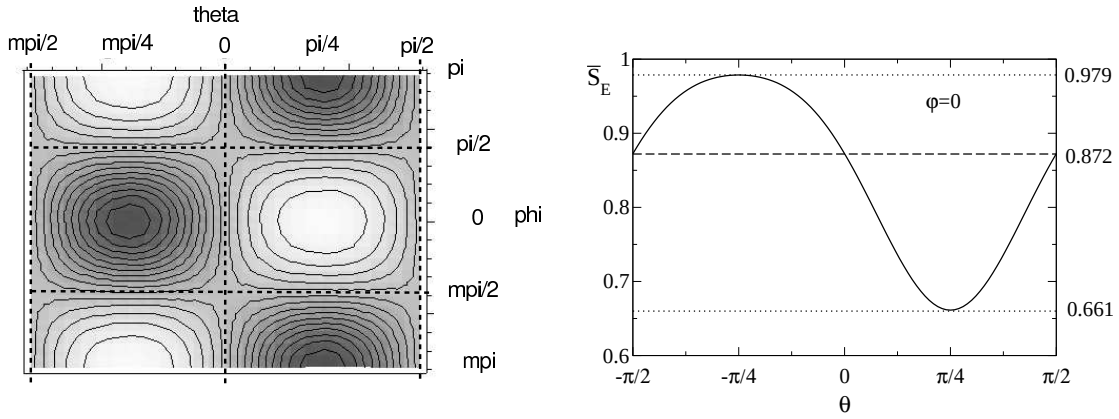

Figure 2. (Left) contour plot of the asymptotic entanglement for non-local initial conditions obtained from eq. (15). Clear areas indicate maxima and dark areas, the minimum values. (Right) variation of asymptotic entanglement with non-locality θ for the particular relative phase $\varphi = 0$.

2.2. Non-local initial coins

In order to explore the effects of non-locality in the initial conditions, let us consider a generic ket in the position subspace spanned by the eigenkets $\|\pm 1\rangle$,

$$|\Psi(\theta,\varphi)\rangle = \left[\cos\theta\,\|-1\rangle + e^{-i\varphi}\sin\theta\,\|1\rangle\right] \otimes |\chi_0\rangle. \tag{13}$$

where the parameters $\theta \in [-\pi/2, \pi/2]$ and $\varphi \in [-\pi, \pi]$ are real angles. The initial coin is fixed at

$$|\chi_0\rangle = \frac{|0\rangle + i|1\rangle}{\sqrt{2}}. \tag{14}$$

Notice that in this case, localized states ($\theta = 0, \pm\pi/2$) result in the intermediate entaglement $\bar{S}_E \approx 0.872$. With these initial conditions, exact asymptotic expressions for the coefficients defined in eqs. (9) can be obtained (again, for the details see Ref. [6]) leading to the eigenvalues

$$\bar{r}_{1,2} = \frac{1}{2} \pm \left[(B_0 - B'\sin 2\theta\cos\varphi)^2 + B_+^2\sin^2 2\theta\sin^2\varphi\right]^{1/2} \tag{15}$$

where $B_0 = (\sqrt{2}-1)/2$, $B' = (3\sqrt{2}-4)/2$ and $B_+ = (\sqrt{2}-1)^2/2$. From this expression, the asymptotic entropy of entanglement $\bar{S}_E(\theta,\varphi)$ can be evaluated exactly. The left panel of Fig. 2 shows a contour plot of this surface. For the initial conditions $(\|-1\rangle \pm \|1\rangle)/\sqrt{2}$, the asymptotic entanglement is maximum $\bar{S}_E \approx 0.979$ or minimum $\bar{S}_E \approx 0.661$, respectively. The vertical dashed lines indicate initially localized position eigenstates and the horizontal dashed lines indicate initial position eigenstates with relative phase $\varphi = \pm\pi/2$. In both cases, the intermediate asymptotic entanglement $\bar{S}_E \approx 0.872$ results. The right panel of Fig. 2 shows the variation of $\bar{S}_E$ with non-locality θ in the particular case when the relative phase is fixed at $\varphi = 0$.

The minimum entanglement that can be obtained from non-local initial conditions in this subspace ($\bar{S}_E \approx 0.661$) is lower than the one attainable from local initial conditions ($\bar{S}_E \approx 0.736$, see Fig. 1). This raises a question about if further non-locality will result in even lower asymptotic entanglement levels. To illustrate the point,

consider an initial Gaussian wave packet with a characteristic spread $\sigma \gg 1$ in position space, with the same coin state $|\chi_0\rangle$ as before. In this case, the Fourier transformed coefficients, $\tilde{a}_k(0) \propto \sqrt{\sigma}\, e^{-k^2\sigma^2/2}$, describe a localized state in k-space. In fact, $\lim_{\sigma\to\infty} |\tilde{a}_k(0)|^2 = 2\pi\delta(k)$, where $\delta(k)$ is Dirac's delta function. In this limit, the eigenvalues of ρ_c reduce to 0 and 1 and the corresponding asymptotic entropy of entanglement becomes vanishingly small. Thus, for a particular uniform initial distribution in position space, a product state results in the long time limit if the appropriate relative phases are chosen.

3. Two entangled walkers

Entanglement in two-particle quantum walks [14, 15, 16, 17] has not been fully characterized yet. The Hilbert space for two walkers is just the tensor product of two one-particle spaces, $\mathcal{H}_{AB} = \mathcal{H}_A \otimes \mathcal{H}_B$, where both $\mathcal{H}_A$ and $\mathcal{H}_B$ are isomorphic to the one-particle space $\mathcal{H} = \mathcal{H}_C \otimes \mathcal{H}_P$ described in Section 2. We label the positions of the walkers with pairs of integers (x, y), so that a generic two-particle pure state $|\Psi\rangle$ is

$$|\Psi\rangle = \sum_{x,y} \{\alpha_{x,y}|00\rangle + \beta_{x,y}|01\rangle + \gamma_{x,y}|10\rangle + \delta_{x,y}|11\rangle\} \otimes \|x, y\rangle \tag{16}$$

with complex coefficients satisfying the normalization requirement

$$\sum_{x,y} |\alpha_{x,y}|^2 + |\beta_{x,y}|^2 + |\gamma_{x,y}|^2 + |\delta_{x,y}|^2 = 1. \tag{17}$$

The two-particle evolution operator is composed of a unitary operation U_C in the two-qubit coin subspace $\mathcal{H}_C^{\otimes 2}$, followed by a conditional shift S in position space,

$$U_{AB} = S \cdot (I_P \otimes U_C) \tag{18}$$

where I_P is the identity in the two-particle position subspace $\mathcal{H}_P^{\otimes 2}$. The shift operator

$$\begin{aligned} S \;=\; & \sum_{x,y} \{|x+1, y+1\rangle\langle x, y| \otimes |00\rangle\langle 00| + |x+1, y-1\rangle\langle x, y| \otimes |01\rangle\langle 01| \\ & + |x-1, y+1\rangle\langle x, y| \otimes |10\rangle\langle 10| + |x-1, y-1\rangle\langle x, y| \otimes |11\rangle\langle 11|\} \end{aligned} \tag{19}$$

performs single-step conditional displacements. An initial two-particle pure state, characterized by a density operator $\rho(0) = |\Psi(0)\rangle\langle\Psi(0)|$, evolves to

$$\rho(t) = U_{AB}^t\, \rho(0) \left(U_{AB}^\dagger\right)^t \tag{20}$$

after t time steps. The resulting joint probability distribution for finding walker A at site x and walker B at site y, is

$$P_{AB}(x, y; t) = tr_C(\rho) = |\alpha_{x,y}|^2 + |\beta_{x,y}|^2 + |\gamma_{x,y}|^2 + |\delta_{x,y}|^2. \tag{21}$$

Note that, if ρ describes a pure, separable state (i.e. $\rho = \rho_A \otimes \rho_B$), the joint distribution is a product of the two single particle distributions, $P_{AB}(x, y; t) = P_A(x, t)P_B(y, t)$. In the generic case, ρ describes an entangled state and a measurement of the position of one walker will affect the position of the other. In this initial work, we restrict consideration to pure states, since the quantification of entanglement in mixed states is more involved.

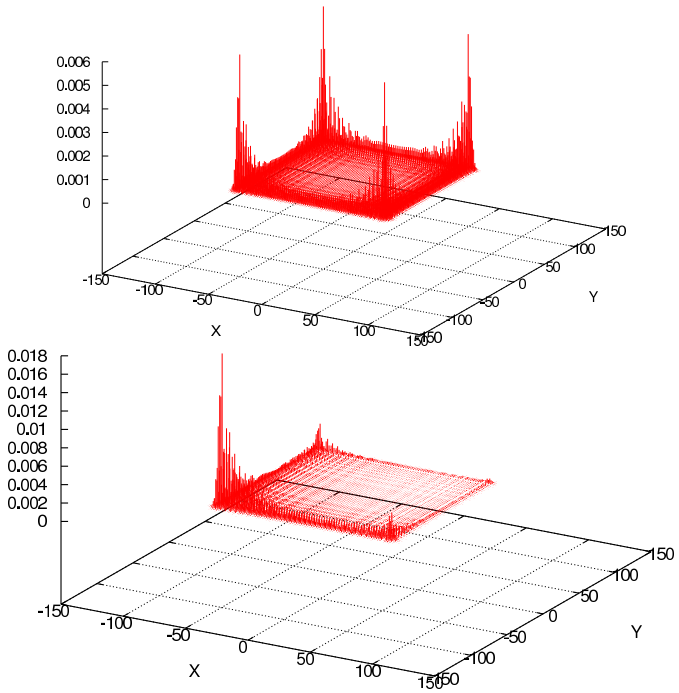

Figure 3. DRAFT Probability distribution $P(x, y)$ after $t = 100$ steps with the separable Hadamard coin, eq. (22). (Left) Initial coins $|\chi_1\rangle$, eq. (23), which result in a symmetrical evolution, i.e. $P_A(x, t) = P_A(-x, t)$ and $P_B(y, t) = P_B(-y, t)$; (Right) Initial coins $|\chi_2\rangle$, eq. (24). In both cases, there is no entanglement between A and B.

3.1. Separable coin operations

In the simplest case, the coin operation U_C in eq. (18) may be separable,

$$U_C = U_A \otimes U_B,$$

where U_A and U_B are local unitary operators in $\mathcal{H}_C$. For these coin operations, entanglement between subspaces $\mathcal{H}_A$ and $\mathcal{H}_B$ can arise only from the choice of initial conditions and it is left unchanged by the evolution. As a simple example, let us consider the two–particle Hadamard walk with

$$U_C = H \otimes H = \frac{1}{2} \begin{pmatrix} 1 & 1 & 1 & 1 \\ 1 & -1 & 1 & -1 \\ 1 & 1 & -1 & -1 \\ 1 & -1 & -1 & 1 \end{pmatrix}. \tag{22}$$

Figure 3 shows the probability distribution obtained after $t = 100$ steps, from two initial initial conditions localized at the origin with the balanced coins

$$|\chi_1\rangle = \frac{1}{2}\left[|00\rangle + i|01\rangle + i|10\rangle - |11\rangle\right] \tag{23}$$

$$|\chi_2\rangle = \frac{1}{2}\left[|00\rangle - |01\rangle - |10\rangle + |11\rangle\right]. \tag{24}$$

Note that both coins are separable so that in this case there is no entanglement between the two particles.

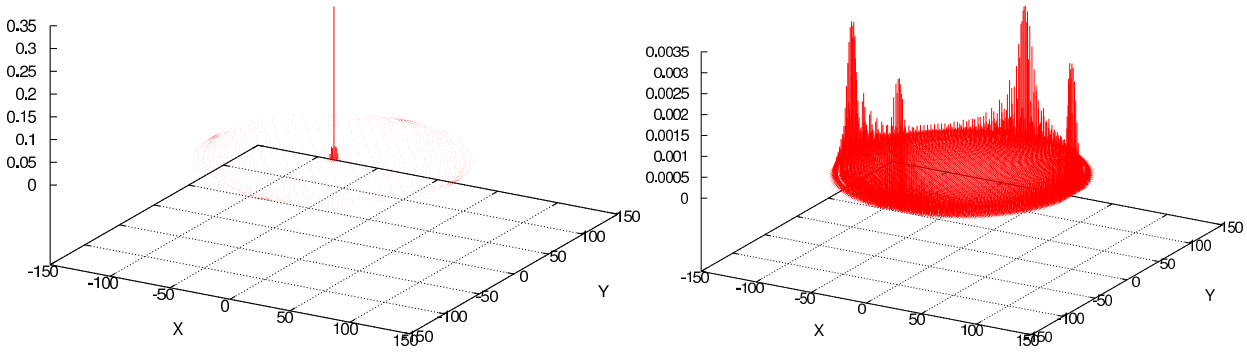

Figure 4. DRAFT Probability distribution $P(x, y)$ after $t = 100$ steps with Grover' s coin, eq. (25). (Left) Initial coins $|\chi_1\rangle$, eq. (23), which results in a distribution which remains highly peaked at the origin; (Right) Initial coins $|\chi_2\rangle$, eq. (24), which results in maximum spread.

3.2. Non-separable coin operations

A more interesting situation is the case of non-separable coins which may change the entanglement between the A and B subspaces. Now entanglement may be introduced by the initial condition or by the coin operation. There are now several kinds of entanglement, since the shift operation still entangles the coin and position degrees of freedom as described in the previous section. We shall consider the entanglement between both particles, generated by the coin operation U_C, thus we use unentangled initial coins from eqs. (23) and (24).

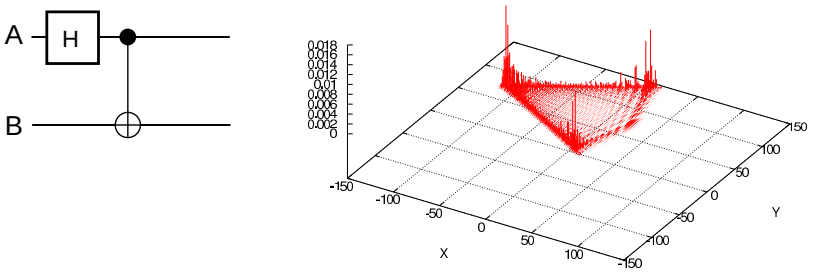

Figure 5. (Left) Schematic diagram showing the action of the coin operation (26) in two-qubit space; (Right) Probability distribution $P(x, y)$ after $t = 100$ steps with the coin operaton defined in eq. (26) corresponding to a Random-Pavlov quantum game. The initial state is localized with coins $|\chi_1\rangle$, eq. (23).

As a first example of non-separable coin operator, consider Grover's coin

$$G = \frac{1}{2}\begin{pmatrix} -1 & 1 & 1 & 1 \\ 1 & -1 & 1 & 1 \\ 1 & 1 & -1 & 1 \\ 1 & 1 & 1 & -1 \end{pmatrix} \tag{25}$$

which plays a central role in Grover's search algorithm [18]. The probability distribution corresponding to this coin operation remains strongly peaked at the origin for most initial coins, see Fig. 4, left panel. However, for the specific initial coin $|\chi_2\rangle$, eq. (24), the distribution has a maximum spread [17], see right panel.

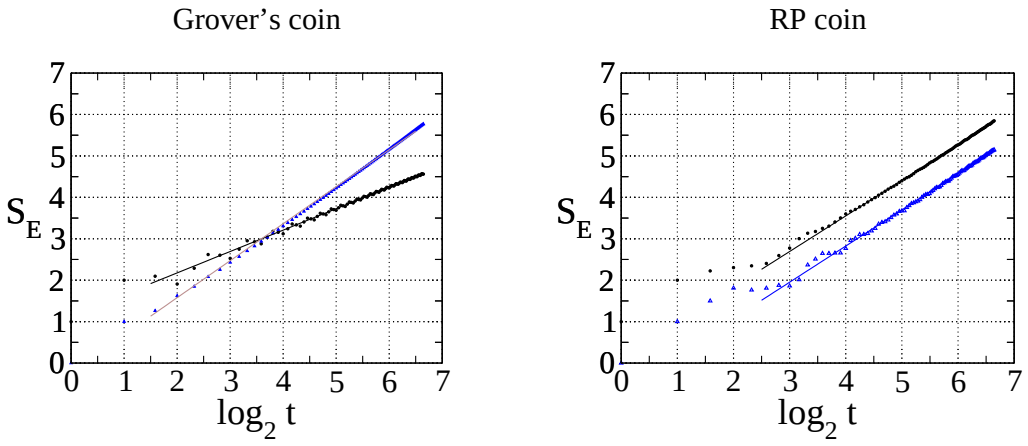

Figure 6. (color online) Entropy of entaglement S_E vs $log_2(t)$ for Grover's coin operation (left panel) and RP coin operation (right panel). Two initial states corresponding to localized states with coins $|\chi_1\rangle$ (black circles) and $|\chi_2\rangle$ (blue triangles) are shown. The straight lines are the linear regression fits as discussed in the text.

Another example of considerable interest is provided by the coin operations associated to quantum strategies in bi-partite quantum games [19]. In particular, the coin operation

$$U_C = CNOT \cdot (H \otimes I) = \frac{1}{\sqrt{2}} \begin{pmatrix} 1 & 0 & 1 & 0 \\ 0 & 1 & 0 & 1 \\ 0 & 1 & 0 & -1 \\ 1 & 0 & -1 & 0 \end{pmatrix} \tag{26}$$

describes a quantum game (RP) in which agent A implements a Random-like strategy, represented by a Hadamard operation H and B responds with a particular Pavlovian strategy (using a CNOT gate). Note that this coin operation, described by the circuit in Fig. 5 (left), generates the Bell states from the computational basis states. The resulting probability distribution (right panel) has a triangular form in (x, y) space.

The time dependence of the bi-partite entanglement generated by the Grover and RP coin operations, quantified with the entropy of entanglement S_E, is shown in Fig. 6. It increases logarithmically with the number of iterations, namely $S_E \sim log_2(t^c)$. This may be associated to the fact that more sites on the plane become occupied and more position eigenstates become entangled as time increases. We estimated the constant c using a linear regression. For Grover's coin operation with initial coin $|\chi_1\rangle$, which leads to minimum spread, $c = 0.52$. In the case of the initial coin $|\chi_2\rangle$, which leads to maximum spread, the entanglement increases faster and $c = 0.89$. The RP coin, while producing a very different spatial distribution, generates entanglement (for both initial conditions) with $c = 0.87$, which is a very similar rate to that of Grover's coin in the maximally spreading case. These linear fits are the straight lines shown in Fig. 6.

4. Conclusions

The evolution operator of the QW generates different kinds of entanglement. The conditional shift operation entangles the coin and position degrees of freedom of each walker.

This kind of entanglement has a well defined asymptotic value that depends on the initial conditions. In the case of a Hadamard walk with spatially localized initial conditions, the asymptotic entanglement varies between almost full entanglement and a minimum entanglement of $\bar{S}_E \approx 0.736$. However, when non-local initial conditions are considered, any asymptotic entanglement level may be obtained.

When two quantum walkers with a non-separable coin operation are considered, the inter-particle entanglement increases at a logarithmic rate. The time dependence of the entanglement generated by Grover's coin and by the RP coin (associated to a particular strategic choice in bi-partite quantum games) has been considered for two initial coins. In most of the cases, the entanglement increases as $S_E \sim \log_2 t^c$ with $c \approx 0.9$. However, for Grover's coin operation with the initial coin $|\chi_1\rangle$ (which leads to a localized probability distribution), the entanglement increases more slowly, with $c = 0.52$. Entanglement is a basic resource in quantum algorithms, and further work is required in order to fully understand its properties in the QW. The analytical method outlined in Section 2 for the case of a single walker, may be extended to the case of two walkers and this should provide a more profound understanding of the time dependence we have described in Section 4 of this work.

Akwnowledgements. *Work supported by PEDECIBA and PDT under project 29/84 (Uruguay). R.D. acknowledges support from CNPq and FAPERJ (Brazil).*

References

[1] Y. Y. Aharonov, L. Davidovich, and N. Zagury, Phys. Rev. A **48**, 1687 (1993).

[2] J. Kempe, Contemp. Phys. **44**, 307 (2003), e-print quant-ph/0303081.

[3] N. Shenvi, J. Kempe, and B. Whaley, Phys. Rev. A **67**, 052307 (2003).

[4] A. Childs *et al.*, Exponential algorithmic speedup by quantum walk, in *Proc. 35th ACM Symposium on Theory of Computing (STOC 2003)*, pp. 59–68, 2003, e-print quant-ph/0209131.

[5] V. Kendon and W. Munro, e-print quant-ph/042140.

[6] G. Abal, R. Siri, A. Romanelli, and R. Donangelo, Phys. Rev. A **73**, 042302, 069905(E) (2006), e-print quant-ph/042140.

[7] A. Romanelli *et al.*, Phys. A **338**, 395 (2004), e-print quant-ph/0310171.

[8] A. Romanelli, R. Siri, G. Abal, A. Auyuanet, and R. Donangelo, Phys. A **347**, 137 (2004), e-print quant-ph/0403192.

[9] C. Bennett, H. Bernstein, S. Popescu, and B. Schumacher, Phys. Rev. A **53**, 2046 (1996).

[10] G. Myhr, Measures of entanglement in quantum mechanics, Master's thesis, NTNU, 2004, arXiv e-print quant-ph/0408094.

[11] V. Vedral and M. Plenio, Phys. Rev. A **57**, 1619 (1998).

[12] Schlientz and G. Mahler, Phys. Rev. A **52**, 4396 (1995).

[13] A. Nayak and A. Vishwanath, e-print quant-ph/0010117.

[14] I. Carneiro *et al.*, New J. Phys. **7**, 156 (2005), e-print quant-ph/0504042.

[15] T. Mackay, S. Bartlett, L. Stephenson, and B. Sanders, J. Phys. A **35**, 2745 (2002), e-print quant-ph/108004.

[16] Y. Omar, N. Paunkovic, L. Sheridan, and S. Bose, arXiv e-print quant-ph/0411065.

[17] B. Tregenna, W. Flannagan, R. Maile, and V. Kendon, New. J. Phys. **5**, 83 (2003), e-print quant-ph/0304204.

[18] L. Grover, in *Proc. 28th ACM Symposium in the Theory of Computation*, pp. 212–219, ACM Press, New York, 1996.

[19] G. Abal, R. R. Donangelo, and H. Fort, Conditional quantum walk and iterated quantum games, in *Annais do* 1^{st} *Workshop-Escola de computacao e Informacao Cuántica, WECIQ06*, PPGINF-UCPel, 2006, quant-ph/0607143.